

NICHT-EBENER RISSFORTSCHRITT MIT DER MIXED-ELEMENTEN-METHODE

D. Bremberg, G. Dhondt

MTU Aero Engines
Postfach 50 06 40
D-80976 Munich
Germany

Zusammenfassung: Ein Rissfortschrittsprogramm, das einen Mixed-Elemente Ansatz benutzt, wurde entwickelt. Zwei schubbelastete Proben wurden geprüft. Die resultierenden K-Verteilungen wurden mit empirischen und numerischen Daten verglichen. Es gab eine gute Übereinstimmung mit anderen bestehenden Programmen. Schließlich wurde eine 3-Punkt Biegeprobe mit 45 Grad schrägem Riss analysiert.

Stichwörter: Mixed-Mode, Rißfortschritt, FEM

OUT-OF-PLANE CRACK GROWTH USING THE MIXED ELEMENT APPROACH

Abstract: A tool for crack growth calculations that uses a mixed element method is under development. Initial evaluations and comparisons to existing tools show promising results. Cracks in two example structures exposed to shear loading are examined. The resulting stress intensity factor distribution is compared to empirical results and numerical results from existing software. It can be seen that the distributions agree well to the available data. A numerical crack growth analysis is performed for a three point bending specimen with a 45 degree inclined crack.

Keywords: Mixed-Mode, Crack propagation, FEM

Introduction

Real life structures are exposed to a combination of complex loading cases on a daily basis. The failure of a structural component may lead to economic damage or even the loss of human lives. Therefore, life assessment becomes very important for some engineering fields and applications.

The reason for failure varies. Most of the time a crack is introduced unintentionally e.g. during manufacturing or as a result of fretting or wear. Once a crack is introduced, cyclic loading may lead to crack propagation and eventually failure. Since crack growth can evolve undetected, good tools are needed during development of new components or for evaluating exposed components.

It has proven far more difficult to predict crack growth in 3-D than in 2-D. The extra

degrees of freedom involve problems that are difficult to take into account for one and the same numerical approach. Analysis tools are used every day but they seem to impose restraints on the analyses. One example is where out-of-plane crack growth is limited to stay in-plane which naturally cannot resemble the real scenario.

The key to good crack growth predictions is that the computations are versatile, automatic and accurate. Users should not need to spend much time in order to perform crack growth analyses, here versatility refers to mesh compatibility. Since the numerical analysis consists of many iterations, the user should not need to intervene during an analysis except for the preparations and retrieving the results. The versatility and automatic nature are important but must not influence the accuracy of the results.

At MTU Aero Engines in Munich, a program named CRACKTRACER [1] is used on a daily basis. It predicts crack growth for complex geometries with the possibility of treating complete missions. It does however restrict the crack to grow in-plane. Since the geometries at hand are not simple, the loading conditions tend to be of a mixed-mode nature. As the program restricts the crack from growing out-of-plane, there is a risk that the result may end far from reality. If the present approach can simulate accurate crack growth in an automatic nature, mixed-mode crack propagation calculations will be within reach.

Automatic crack insertion

The starting point is a structure, an initial crack plus boundary conditions and loads. A tube-shaped domain along the crack front is identified and filled with a mapped mesh. The tube shaped mesh consists of standard quadratic hexahedral elements which in the innermost layer are turned into collapsed quarter point elements. A quadratic tetrahedral mesh fills the remaining structure. The two separate meshes are connected with linear constraint equations. This method yields accurate calculations thanks to the mapped mesh about the crack front and the good meshing capabilities due to the tetrahedral mesh. A thorough description of the method can be found in [2].

The cracked mesh, see Figure 1, will not equal the initial structure mesh. Loads and boundary conditions are all defined for the initial mesh and therefore have to be transferred to the cracked mesh. Examples of entities that have to be transferred are temperature, concentrated loads and single point constraints (SPC). The temperature of the cracked mesh nodes are interpolated while the concentrated loads are redistributed. A single point constraint is turned into an MPC by copying the SPC node to the cracked mesh and using it in an MPC equation together with the corresponding nodes of the cracked mesh.

Stress intensity factor evaluation

Once the loads and boundary conditions are transferred from the initial mesh to the cracked mesh, the global stress field is computed by use of a generic finite element (FE) solver. The stress field near the crack front exhibits a $1/r^{1/2}$ -singularity due to the characteristics of the collapsed quarter point elements [3]. Comparing this asymptotic stress field at the integration points to the analytical expressions, one arrives at the desired stress intensity factors (SIF). This rests on the assumption that a 2-D approximation of the stress state is allowed. However, this assumption is not valid

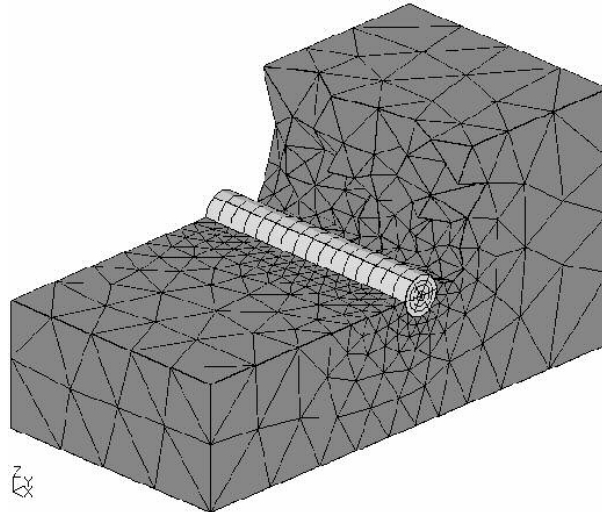


Figure 1. The cracked mesh of a SEN specimen where the top left part of the mesh has been removed. The flat top surface of the bottom left part is the lower crack face. The hexahedral mesh enclosing the crack front is clearly visible.

close to the free boundary which locally influences the stress field. It is expected that this area is very small and probably does not contain any or only very few integration points. The influence can therefore be neglected.

The next step is to derive an equivalent stress intensity factor. This is done using one of the available 3-D criteria e.g. the criteria by Sih [4], Pook [5,6], Schöllman et al [7,8], Richard [9] or Dhondt [10].

In addition to the equivalent stress intensity factor also one or more deflection angles are calculated. The most important deflection angle is the one describing the kinking of the crack and thus the propagation direction. All deflection angles and stress intensity factors are smoothed in order to eliminate large local variations along the crack front.

Crack growth calculation

The equivalent K-factor and the deflection angle must be translated into a crack growth that can be accumulated for each iteration. In order to retrieve a smooth crack growth in not too big increments, the growth magnitude and the deflection of the crack are restricted. The crack growth increment due to one load cycle is calculated with some crack propagation law, e.g. Paris' law. Here, a slightly modified Paris' law is used taking into account the effect of threshold values and unstable growth. When the new crack front is calculated it is smoothed before it is connected to the previous crack front. The iterative process either restarts or comes to a halt according to a stop criterion. A suitable stop criterion could for instance be when there is no crack growth or if the growth exceeds a predefined threshold value.

K-distributions

Crack propagation calculations must be correct, no matter how fancy the preprocessing steps may be. It is therefore a good start to compare the results from the new approach with existing software and empirical findings at an early stage. The results to compare could for instance be the stress field along the crack front and subsequently the SIFs. The SIFs along the crack front are compared between the

present method and CRACKTRACER. Two example structures are treated [11], a quarter circular corner crack specimen (QCCC) and a single edge notch specimen (SEN), see Figure 2. Both structures have a simple geometry in which initial cracks are inserted. The structures are exposed to prescribed shear loading, see Figure 3.

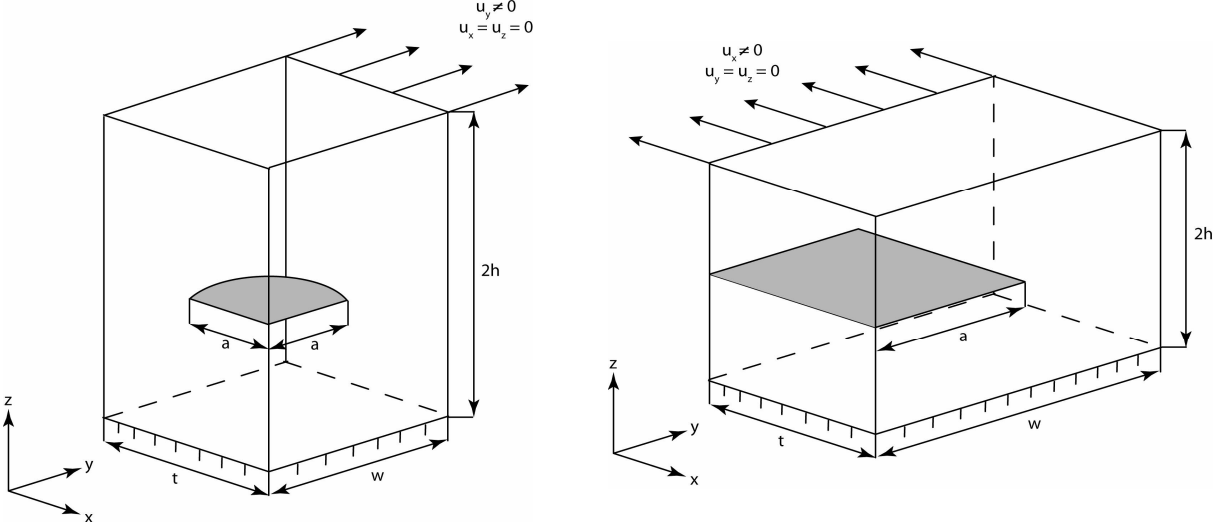


Figure 2. The shear loading of the QCCC and SEN specimens.

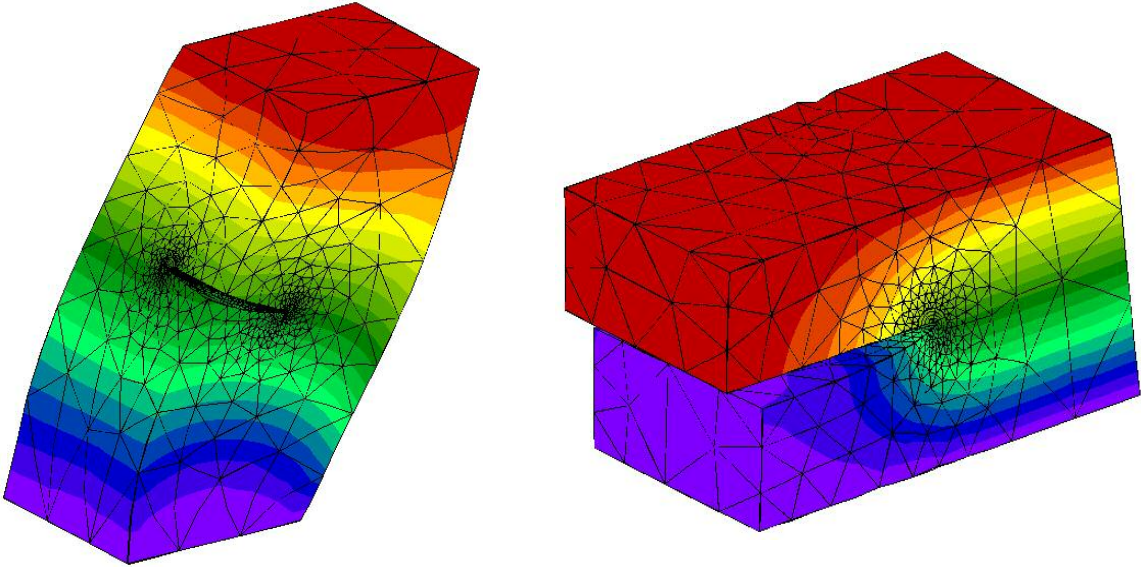


Figure 3. Magnified deformation of the QCCC and SEN specimens.

Due to the shear loading, it is expected that the resulting K-distributions exhibit strong mixed-mode features. Both cases can be found in the literature [12] for comparing the numerical results to experimental findings, see Figure 4 and 5.

It should be noted that the SIF distribution for the SEN specimen is symmetric about the centre of the crack front. This is not the case for the QCCC specimen due to the curved crack front. This means that the SEN specimen yields a crack growth that is anti-symmetric about half the crack length. For the QCCC specimen the deflection is stronger in the end of the of the crack front than in the beginning.

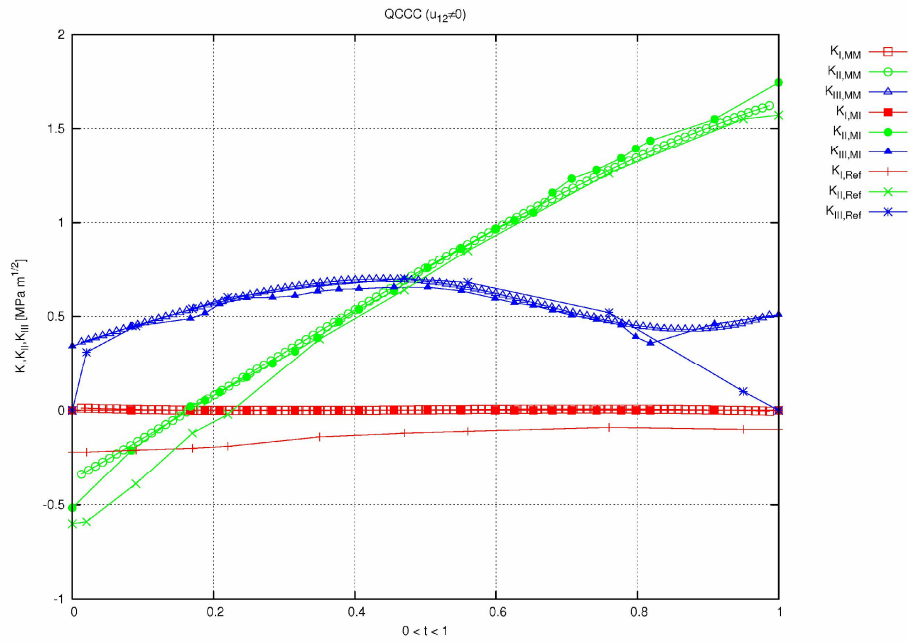


Figure 4. The stress intensity factor distribution from the QCCC specimen for the proposed method (MM), CRACKTRACER (MI) and the empirical data (Ref).

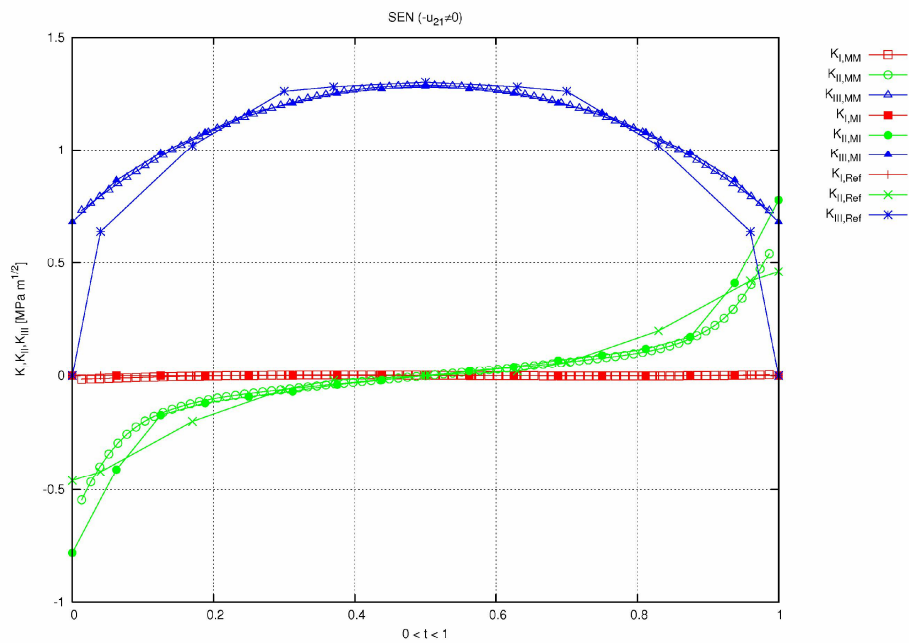


Figure 5. The stress intensity factor distribution from the SEN specimen for the proposed method (MM), CRACKTRACER (MI) and the empirical data (Ref).

Crack propagation in a three point bending specimen

A popular method of generating mixed-mode crack propagation in an easy way is to analyse a three point bending specimen with a 45 degree inclined initial crack. It is expected that the crack will grow towards the loading symmetry and hence grow out-of-plane. In the beginning mode-II and mode-III dominates the crack growth but mode-I takes over as the crack propagates. The initial crack front is straight but quickly becomes curved due to the mixed-mode properties of the loading. Figure 6 shows the crack after 50 iterations.

In the centre, however, the crack will not bend but grow straight ahead. The result is a twisted crack as if a torque is applied, see Figure 8. This agrees to the experimental findings available. Figure 9 shows a titanium three point bending specimen with an initially 45 degree inclined crack with a straight crack front. The figure reveals a non-smooth crack growth where facets are formed, normally referred to as factory rooftop. It is unclear why this occurs but it is argued that the strong mode-III contributes. This phenomenon is very difficult to catch with a numerical tool. The second deflection angle describing the angle of the factory roof can be calculated but the difficulty lies in telling where and how far each facet evolves.

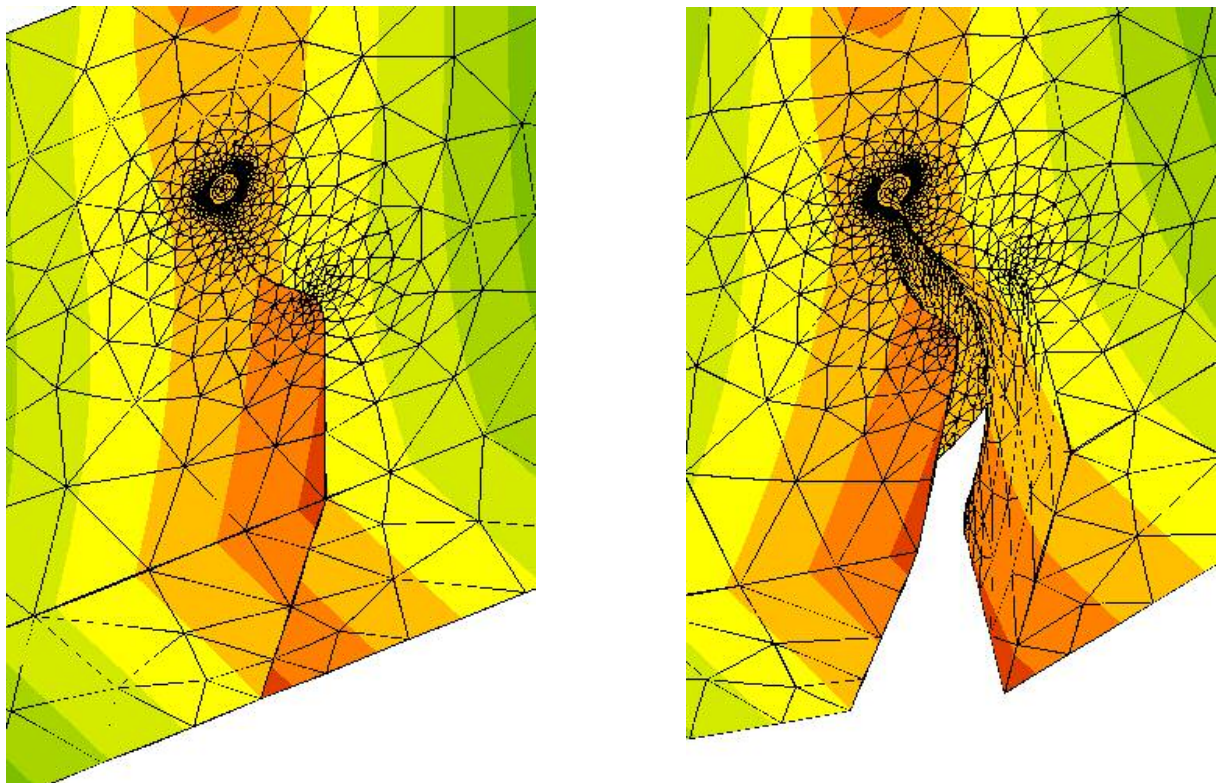


Figure 6. The evolved crack is visible but becomes even more clear if the displacement is magnified.

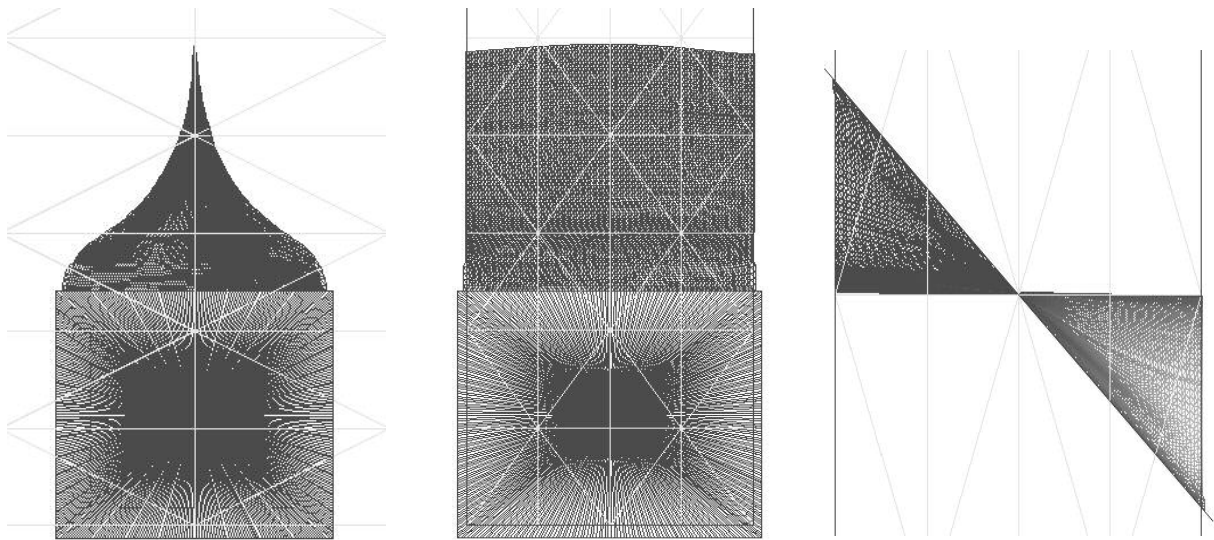


Figure 7. The accumulated crack fronts as a front view, side view and top view, respectively.

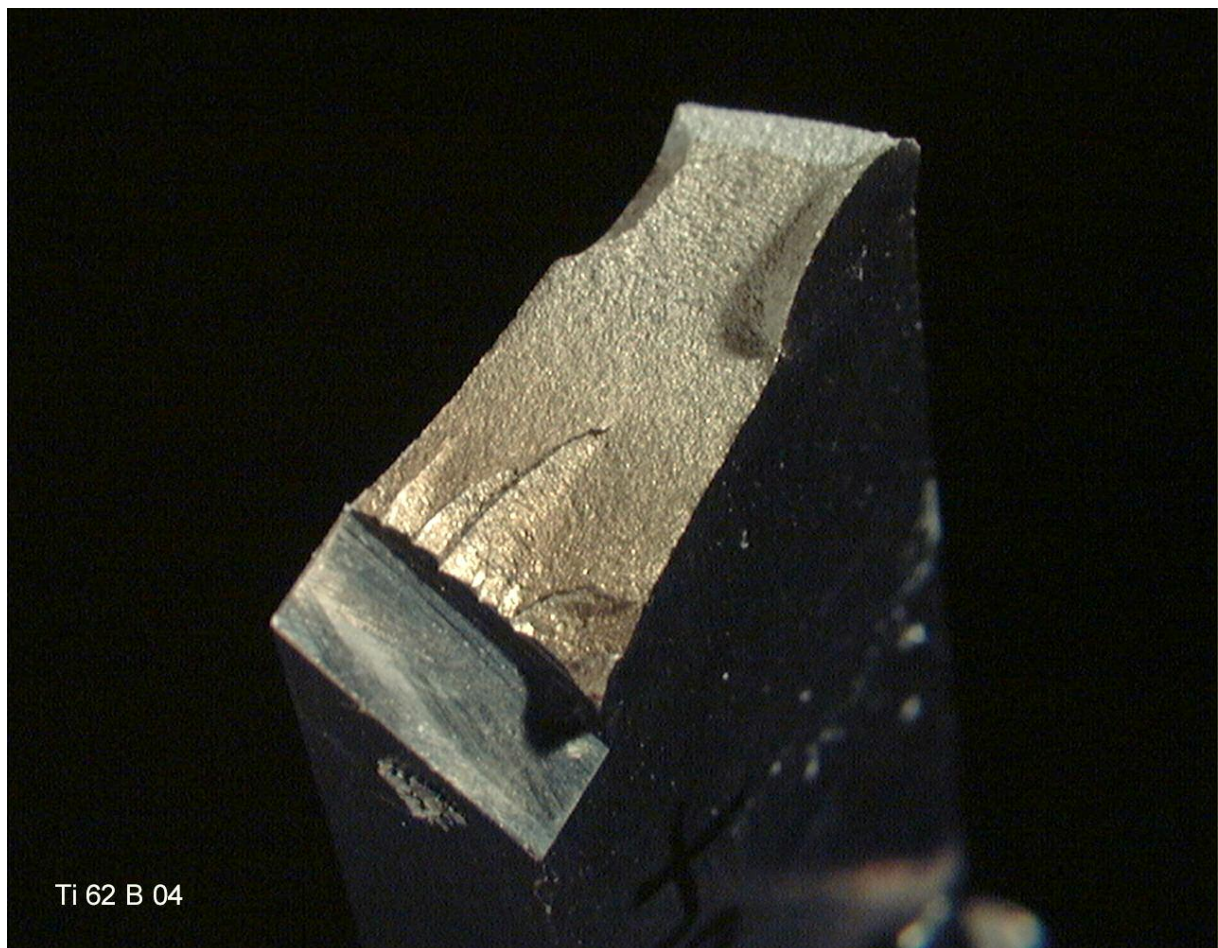


Figure 8. A three point bending specimen with a crack face that reveals the factory roof at the beginning of the crack growth.

Summary

There are many ways in which mixed-mode crack growth can be calculated. All of which impose restrictions on the analysis in one way or the other. A new approach that strives towards versatility and accuracy is being investigated. As the development proceeds it is important to evaluate the results. It has been shown that challenging examples can be generated with simple structures and crack configurations. Using these examples, a comparison between the results from the new approach and available numerical and empirical studies shows that the results are in close agreement. It is important that the correctness in crack growth path and loading cycles is ensured. Therefore, the next step will be to evaluate the results from full crack growth analyses.

References

1. Dhondt, G. (1999) Design principles and methods for aircraft and gas turbine engines. In: RTO Meeting Proceedings 8.
2. Bremberg, D, Dhondt, G. (2008). Eng. Frac. Mech. 75, 404-416.
3. Dhondt, G. (1993). Int. J. Num. Meth. Engng. 36, 1223-1243.
4. Sih, G. C. (1979). Int. J. Frac. 10, 305-321.
5. Pook, L. P. (1980). In: Fracture and Fatigue: Elasto-Plasticity, Thin Sheet and Micromechanism Problems, pp. 143-153, Radon, J.C. (Ed.) Pergamon Press, Oxford.
6. Pook, L. P. (2000). Linear elastic fracture Mechanics for engineers: theory and application. WIT press, Southampton.
7. Schöllmann, M., Richard, H. A., Kullmer, G. and Fulland, M. (2001). Proc. Of 6th Int. Conf. Of Biaxial/Multiaxial Fatigue & Fracture, Vol. 2, 589-596.
8. Schöllmann, M., Fulland, M. and Richard, H. A. (2002). Int. J. Frac. 117, 129-141.
9. Richard, H. A. (2001). In: CD-Rom Proceedings of ICF10, Honolulu USA.
10. Dhondt, G. (2003). Key Engineering Materials, Vols. 251-252, pp. 209-214.
11. Dhondt, G., Chergui, A., Buchholz, F. G. (2001). Eng. Frac. Mech. 68, 383-401.
12. Murakami, Y. (1987). Stress intensity factors handbook. Oxford: Pergamon Press.